GEOLOGY

# Evaporative fractionation of zinc during the first nuclear detonation

James M. D. Day,[1,2]* Frédéric Moynier,[2] Alex P. Meshik,[3] Olga V. Pradivtseva,[3] Donald R. Petit[4]



**Volatile element and compound abundances vary widely in planets and were set during the earliest stages of solar system evolution. Experiments or natural analogs approximating these early conditions are limited. Using silicate glass formed from arkosic sands during the first nuclear detonation at the Trinity test site, New Mexico, we show that the isotopes of zinc were fractionated during evaporation. The green silicate glasses, termed "trinitite," show +0.5 ± 0.1‰/atomic mass unit isotopic fractionation from ~200 m to within 10 m of ground zero of the detonation, corresponding to an α fractionation factor between 0.999 and 0.9995. These results confirm that Zn isotopic fractionation occurs through evaporation processes at high temperatures. Evidence for similar fractionations in lunar samples consequently implies a volatile-depleted bulk Moon, with evaporation occurring during a giant impact or in a magma ocean.**

## INTRODUCTION

The inventory of volatile elements and compounds in planetary bodies plays a crucial role in their evolution, fundamentally altering melting and differentiation processes (*1*, *2*), generation and sustainability of atmospheres and oceans (*3*), and planetary habitability. Element volatility is typically defined by the 50% condensation temperature ($TC_{50}$), calculated at a total pressure near 1 astronomical unit ($1.5 \times 10^8$ km) in the solar nebula of $10^{-4}$ bar (*4*). Volatiles include both low–boiling point compounds (for example, $H_2O$, $CO_2$, $CH_4$, $SO_2$, and $NH_3$), as well as elements with atmophile ($TC_{50}$, <200 K; H, C, N, O, and noble gases), highly volatile ($TC_{50}$, <664 K; for example, Cl, S, Se, Sn, and Pb), and volatile to moderately volatile characteristics ($TC_{50}$, 665 to 1134 K; for example, K, Zn, Rb, P, and Cs). Understanding planetary processes requires knowledge of the behavior of volatile elements and compounds and how and when they were added or lost from planetary bodies.

Constraints have been placed on planetary volatile inventories using atmophile elements and water, but these elements and compounds tend to have highly incompatible characteristics during melting of planetary interiors (*5*), becoming ice, liquid, or vapor at planetary surfaces, greatly complicating estimations of planetary volatile inventories. Conversely, many volatile and moderately volatile elements are also lithophile elements, remaining in rock-forming minerals and melts. In particular, the moderately volatile element zinc ($TC_{50}$, 726 K) is a tracer of planetary volatile histories, because it behaves predictably during planetary melting (*6*), and has five stable isotopes ($^{64}Zn$, $^{66}Zn$, $^{67}Zn$, $^{68}Zn$, and $^{70}Zn$), making it possible to investigate kinetic or equilibrium isotopic fractionation effects (*7*) during evaporative fractionation. It has been demonstrated that there is a strong depletion of Zn in the Moon, compared with Earth, implying significant volatile loss during lunar formation (*8*–*10*). However, it has also been shown that Zn isotopic fractionations [expressed as $\delta^{x}Zn = (([^{x}Zn/^{64}Zn)_{sample}/[^{x}Zn/^{64}Zn]_{JMC\ Lyon} - 1) \times 1000$, where $^{x}Zn$ equals either $^{66}Zn$, $^{67}Zn$, $^{68}Zn$, or $^{70}Zn$] of planetary materials do not perfectly match predicted fractionations of the isotopes during kinetic processes but, rather, follow subdued fractionations that approach unity (*6*). Experimental evidence of this effect has yet to be demonstrated for zinc but has been found in potassium, from ~$10^{-9}$ to 1 bar (*11*, *12*), with the results possibly consistent with fractionation factors close to unity at high pressures (*13*).

A major impediment in interpreting volatile element isotope fractionations has been the fact that laboratory experiments are either unable to reproduce the scale or temperatures consistent with planetary-scale volatile processes, or are lacking for many elements, making empirical assessment of isotopic fractionation and volatile element loss challenging. This is a particular problem because studies of volatile compounds, such as water or OH in lunar glasses, suggest that the Moon may have volatile element abundances approaching Earth's upper mantle composition (*14*, *15*); other studies have suggested localized volatile loss from the Moon (*16*), in contrast to the large-scale processes of volatile loss suggested for Zn (*6*, *8*, *9*) and K (*13*).

To empirically constrain the isotopic fractionation factor of Zn and the behavior of moderately volatile elements during evaporative fractionation, we have investigated Zn isotope and trace element abundances in trinitite glasses from the Trinity test site, New Mexico, USA. The Trinity test site was the location of the first nuclear detonation, on 16 July 1945. The $^{239}Pu$ implosion device (Y-1561), known as the "Gadget," exploded with the equivalent force of 84 TJ, creating local conditions at the site of 8430 K and >8 GPa, and localized vaporization of the arkosic desert sand. Vaporization, melting, and redistribution of the sand led to the formation of a thin sheet of dominantly green-colored glass that extended approximately 300 to 350 m from ground zero, beneath the Gadget (*17*). The Trinity test site is a large-scale "experiment" for understanding volatile processes occurring at temperatures and/or pressures relevant to those found during planetary formation.

## RESULTS

Samples investigated in this study include trinitite taken within 10 m of ground zero (IF), at 100 m (IG), and within 150 to 250 m [trinitite 1 (T1), T2, and T3]. For samples IF and IG, Xe isotope abundances were measured, allowing estimation of the cooling rate and temperatures of formation of the glass. The 10 m sample, IF, formed at 1663 K and cooled within 17 min of emplacement, while the 100 m sample, IG, formed at 1593 K and cooled within 5 min of emplacement (*18*). Peripheral samples (T1, T2, and T3) likely formed at lower temperatures and higher rates of cooling, and samples T2 and T3 had

[1]Scripps Institution of Oceanography, University of California, San Diego, La Jolla, CA 92093–0244, USA. [2]Institut de Physique du Globe de Paris, Université Paris Diderot, Sorbonne Paris Cité, 1 rue Jussieu, 75005 Paris, France. [3]McDonnell Center for the Space Sciences, Washington University in Saint Louis, Saint Louis, MO 63130, USA. [4]Lyndon B. Johnson Space Center, Houston, TX 77058, USA.
*Corresponding author. Email: jmdday@ucsd.edu

quantities of unmelted desert sand adhering to them. Although maximum conditions at the nuclear test site were exceptionally high (8430 K), we consider the bound of 1663 K as the maximum temperature condition for the formation of the trinitite glasses. By using the Clausius-Clapeyron relationship, this equates to ≤0.2 GPa of vapor pressure in the desert air.

Trinitite samples have similar abundances of refractory elements ($TC_{50}$, >1600 K), regardless of distance from ground zero, save for variations of U and Th abundances (Fig. 1). Trinitite occurs in a variety of colors and differing morphologies, with evidence that red trinitite formed with enhanced abundances of Fe, Cu, and Pb inherited from copper cables, lead bricks, and the iron steel tower holding the bomb casing materials in place at the test site (*19*). Likewise, U, Th, and Pb excesses in some green trinitite glasses have been related to the presence of bomb materials (*20*). Significant differences in Fe, Zn, Se, and Ge abundances occur between the "proximal" 10 m (IF) and 100 m (IG) trinitite glasses, compared with the peripheral trinitite glasses (T1, T2, and T3). Remarkably, Fe is lower in the IF and IG trinitite glasses despite their close proximity to the steel tower that held the Gadget in place, in contrast to the metal-rich red trinitite (*19*).

Zinc isotope and abundance measurements were performed both in bulk samples of trinitite and in leaching and etching experiments to investigate the location of Zn within trinitite samples. Samples T1, T2, and T3 have between 16.3 and 18.3 μg $g^{-1}$ Zn, with $\delta^{66}$Zn values of 0.31 to 0.46‰. Samples IG (100 m) and IF (10 m) have lower Zn abundances (12.6 to 13.2 μg $g^{-1}$) and $\delta^{66}$Zn values of 0.64 and 0.72‰, respectively. In general, hydrochloric acid leachates are significantly isotopically lighter than bulk-rock samples, while the HF-$HNO_3$ etchates, which are interpreted to attack silicate material in the trinitite, are similar in isotopic composition to the bulk samples, as are the residues after etching. Recombination of leachates, etchates, and residues leads to reconstructed bulk compositions that are similar to the measured bulk samples. In a plot of $\delta^{66}$Zn versus $\delta^{68}$Zn, bulk-rock samples, residues, and leachates/etchates fall on a slope of ~2, conforming to mass-dependent fractionation. Water leachates were consistently too low in Zn to accurately measure Zn isotope compositions (Fig. 2).

## Zinc isotope fractionation with distance from the Gadget

A remarkable feature of the Zn isotope compositions of trinitite is that it correlates ($R^2$ = 0.8) with the distance from ground zero at the Trinity test site (Fig. 3). With increasing distance from ground zero, Zn abundances increase and $\delta^{66}$Zn decreases. The least-melted and peripheral trinitite sample (T3) has $\delta^{66}$Zn values similar to those of the arkosic desert sand at ~0.2 to 0.25‰, which is within uncertainty of estimates of terrestrial igneous rocks (*21*). Extrapolation of the trend in $\delta^{66}$Zn versus distance from the Gadget indicates that the average arkosic sand composition is ~0.2‰, consistent with the least-melted trinitite sample. Conversely, $\delta^{66}$Zn values for sample IF, 10 m from ground zero, are between 0.4‰ (bulk versus bulk) and 0.6‰ (residue versus residue) heavier than the least-melted trinitite. Collectively, these results indicate evaporative loss of zinc, as well as of some other volatile elements depleted in the proximal trinitites (Se, Ge, and possibly Fe), with distance from the epicenter of the nuclear detonation. Given these conditions, isotopically light $\delta^{66}$Zn values for leachates can be interpreted as condensate vapor that collected on the trinitite glass during cooling in the aftermath of the nuclear detonation.

## Natural analogs and empirical fractionation factors

Some natural analogs approach conditions required for volatile loss in planets. For this reason, we consider their suitability for calculating empirical fractionation factors. Glasses formed through lightning strikes, called fulgurites, can be formed at reducing conditions at pressures up to 25 GPa and temperatures of 2000 K (*22*); however, fulgurites are also formed locally ($10^0$ to $10^1$ m) and in the ground, potentially leading to chemical buffering effects with the surrounding soil. No data are currently available for these samples for Zn isotopes. Larger-scale natural analogs include tektite glasses. Tektites form through meteoroid collisions with the Earth's atmosphere, leading to extreme heating (>2273 K), pressure (4 to 100 GPa), reduction, and potentially localized atmospheric blow-off (*23*), generating glasses with compositions similar to those of soils (*24*). Tektites show progressive heavy Zn isotope enrichment with decreasing Zn abundance, consistent with fractionation due to evaporation and progressive volatile element loss during their formation (*25*). As with studies of lunar

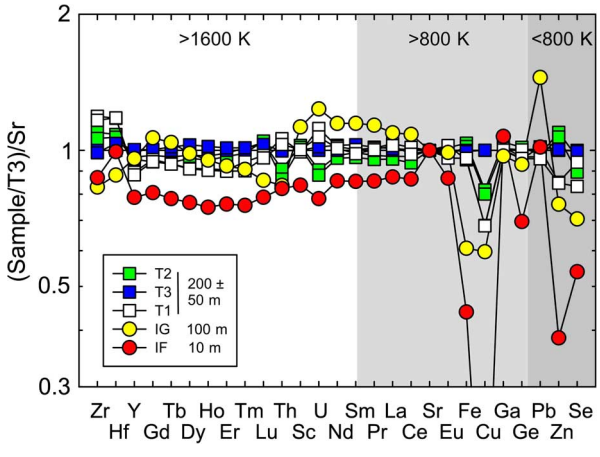


**Fig. 1. Incompatible trace element abundances in trinitite glasses, ordered according to $TC_{50}$, double-normalized over the least-melted trinitite sample (T3) and strontium.** $TC_{50}$ are from a study by Lodders (*4*), with shaded boundaries shown for elements with $TC_{50}$ of >1600, >800, and <800 K.

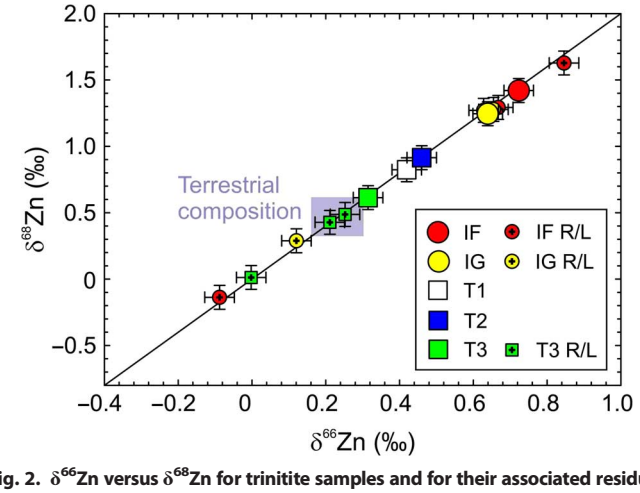


**Fig. 2. $\delta^{66}$Zn versus $\delta^{68}$Zn for trinitite samples and for their associated residues and leachates or etchates.** Solid line illustrates the predicted mass-dependent fractionation curve of 2. Shaded bars define the terrestrial Zn isotope composition from a study by Chen *et al.* (*21*). R, residues; L, leachates or etchates.

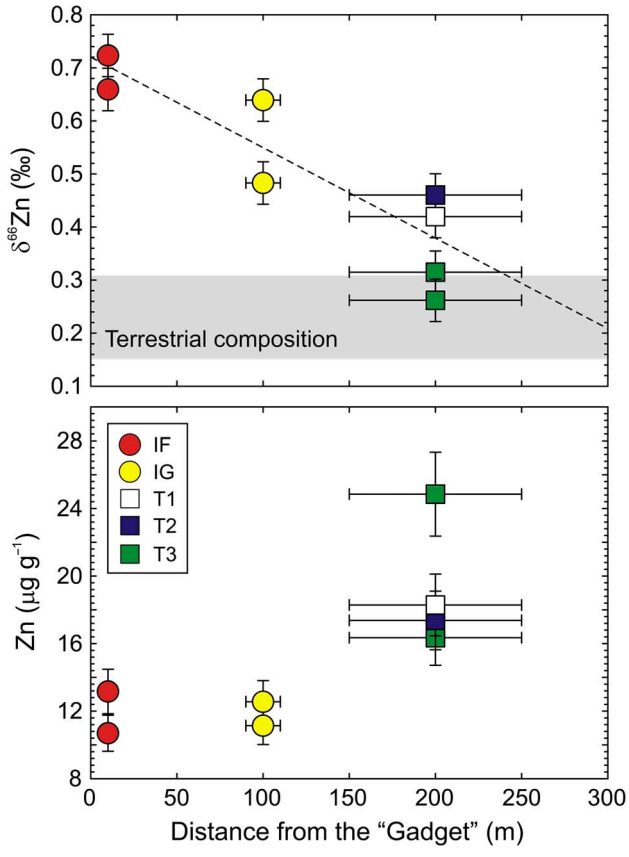


**Fig. 3. Relationship of $\delta^{66}$Zn and Zn abundance in trinitite glasses with distance from the Gadget nuclear device at the Trinity test site.** Relationships of the samples with distance define $\delta^{66}$Zn variation of $-0.0017x + 0.7181$ with an $R^2$ of 0.8 (stippled line).

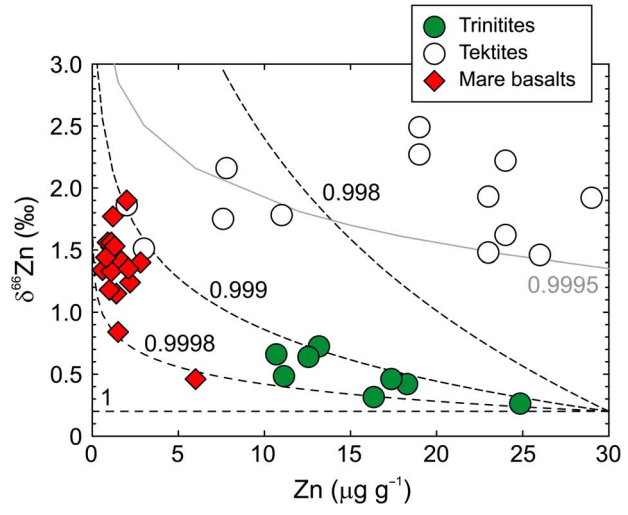


**Fig. 4. Zn abundance versus $\delta^{66}$Zn for trinitite glasses versus tektites and mare basalts [from studies by Paniello *et al.* (*8*), Kato *et al.* (*9*), and Moynier *et al.* (*25*)].** Rayleigh distillation curves are shown for different α fractionation factors (1, 0.9998, 0.999, and 0.998) for arkosic sand at the Trinity test site with 30 μg $g^{-1}$ Zn. Mare basalts fall within the same α curves (0.9998 to 0.999) as trinitite, implying similar, or lower, starting Zn abundances. Also shown is the Rayleigh distillation curve assuming a chondritic abundance of Zn (300 μg $g^{-1}$), which passes through tektites at an α of 0.9995, illustrating that these isotopically fractionated materials likely derived from a higher initial Zn abundance.

rocks (*8*, *9*), tektites do not conform to ideal fractionation behavior, defined by the fractionation (α) factor of different isotopologs of Zn (for example, ZnCl or ZnS), which are typically <0.998. Furthermore, the conditions of evaporation for tektites are not well constrained.

Using the trinitite glasses, it is possible to calculate the empirical fractionation factor during evaporation of Zn at the first nuclear detonation. Rayleigh distillation calculations were performed, assuming a starting composition of 30 μg $g^{-1}$ Zn and $\delta^{66}$Zn of 0.2‰, consistent with the composition of the bulk arkosic sand. Best-fit α factors for the trinitite glasses correspond to values of 0.999 to 0.9998 (Fig. 4). Empirically derived α factors obtained from the trinitite glass at maximum localized conditions of 1663 K (IF) support previous suggestions that the α factor does not approach ideal values estimated from isotopologs because of complex vapor-liquid reactions during evaporative fractionation (*6*). Our data suggest that with an α of 0.9995, it is possible to fit a Rayleigh distillation model to the most Zn-depleted tektites, assuming a high initial Zn abundance (200 to 300 μg $g^{-1}$), consistent with abundances of Zn in isotopically lighter tektites (*25*). The range of fractionation factors for trinitite also encompasses the range of $\delta^{66}$Zn and Zn abundances for lunar mare basalts, supporting low Zn contents in the lunar mantle inferred from Zn/Fe variations (*10*).

### Evaporation of volatile elements from the Moon

The new results from trinitite provide the first definitive evidence for evaporative fractionation of Zn during high-temperature conditions and are consistent with subdued fractionation factors for Zn. Pressure conditions are more difficult to ascertain, but elevated pressures are likely during planetary formation (*13*) or during global magma ocean phases on planetary bodies, when volatile loss led to nascent atmospheres (*6*). These results strongly support the loss of Zn and other volatile and moderately volatile elements through evaporative fractionation effects during the formation and evolution of the Moon, as well as other planetary bodies.

Studies of Zn, Cl, S, and K isotopes in lunar materials (*6*, *8*, *9*, *13*, *16*), OH contents in apatites from lunar mare basalts (*26*), and moderately volatile element abundance in mare basalts (*10*, *27*) imply a volatile-depleted Moon. These results contrast with evidence from the Apollo high-Ti lunar glass 74220 that implies a lunar interior with water contents similar to those of Earth's mantle (*14*, *15*). Mechanisms for evaporative loss of volatile elements consistent with available Zn isotope data include a giant impact (*8*) or loss from a magma ocean (*6*). Possible evidence for isotopically light Zn on the surface of trinitites at the Trinity test site suggests that the latter mechanism would predict the presence of isotopically light condensates on the lunar surface, and more heterogeneous distribution of volatiles within the Moon. In contrast, giant impact evaporative loss would imply homogeneous "dry out" of materials accreting to form the Moon. The evidence for evaporative fractionation of Zn and other volatile and moderately volatile elements, combined with the presence of high water contents in some lunar samples, implicates heterogeneous distribution of volatiles in an otherwise "dry" Moon.

## MATERIALS AND METHODS

### Samples

T1, T2, and T3 are samples from the periphery of the affected blast site, with an estimate distance of 200 ± 50 m. T3 had the least amount of trinitite glass, and we used this sample to estimate background trace

element abundances and $\delta^{66}$Zn at the Trinity test site. The composition of T3 is similar to that reported for "unmelted" sand (*20*). IF1 and IG1 (referred to in the text as IF and IG) are well-characterized samples from 10 and 100 m, respectively, from the location of detonation of the Gadget.

### Leaching and etching experiments

Because of the requirement of assessing elemental and isotopic heterogeneity within fragments of trinitite, we used a systematic leaching and etching procedure. This included crushing and powdering whole-rock samples, with no etching or modification (IF-2 = IF1; IG-2 = IG1; T1 = J8; T2 = J9; T3 = J10). We then took three powdered splits of IF-2 (IFL), IG-2 (IGL), and T3 (TT) and subjected them to a three-step process. Aliquots of the sample powder were first precisely weighed in a Teflon vessel and then subjected to a first-stage leach for 20 min in 18.2-megaohm $H_2O$, with ultrasonification at 30°C. The $H_2O$ leachate was extracted (IFL2, IGL2, and TT2), and 3 M HCl was then added to the residue. The second step was also for 20 min, with ultrasonification at 30°C. The 3 M HCl leach was then extracted from the residue (IFL3, IGL3, and TT3). The final etching stage involved the addition of 1 M HF-$HNO_3$ and etching of the residue for 2 hours on a hot plate at 60°C. After extraction of this final etchate (IFL4, IGL4, and TT4), samples were dried down and weighed before treatment in an identical fashion for dissolution, as described below. These residues are referred to as IFL1, IGL1, and TT1.

### Zinc isotopic and abundance measurements

We used methods for the purification and isotopic measurement of Zn, as described previously (*28*). Samples were dissolved in a 4:1 mixture of ultrapure HF/$HNO_3$ in Teflon beakers for 4 days. Zinc purification was achieved using anion exchange chromatography, with a recovery of 99 ± 1%. The samples were loaded in 1.5 N HBr on 0.25-ml AG-1X8 (200 to 400 mesh) ion exchange columns, and Zn was collected in 0.5 N $HNO_3$. The Zn fraction was further purified by eluting the samples twice on a 100-µl column, with the same eluting solutions. The blank measured with samples was 5 ng, in line with our previous work (*8*, *9*), and generally represents less than 2% of total measured Zn for most samples, except for some of the low–Zn abundance leachates (table S1).

Zinc isotopic compositions were measured on the ThermoElectron Neptune Plus Multicollector Inductively Coupled Plasma Mass Spectrometer, housed at the Institut de Physique du Globe de Paris. The Faraday cups were positioned to collect the masses 62, 63, 64, 65, 66, 67, and 68. Possible $^{64}$Ni isobaric interferences were monitored and corrected by measuring the intensity of the $^{62}$Ni peak. A solution containing 500 parts per billion (ppb) of Zn in 0.1 M $HNO_3$ was prepared for isotopic analysis and was matched with 500-ppb standard solutions. Isotopic ratios of Zn in all samples were analyzed using a spray chamber combined with a PFA nebulizer at 100 µl/min. One block of 30 ratios was collected for each individual sample measurement, in which the integration time of a single scan was 10 s. The background was corrected by subtracting the on-peak zero intensities from a blank solution. Instrumental mass bias was corrected by bracketing each of the samples with standards. External precision based on the JMC Lyon Zn standard was 0.04 ‰/amu (atomic mass unit) (2σ) for $\delta^{66}$Zn and 0.09 ‰/amu (2σ) for $\delta^{67}$Zn and $\delta^{68}$Zn. Values of $\delta^{66}$Zn, $\delta^{67}$Zn, and $\delta^{68}$Zn were found to be within uncertainty for the JMC Lyon Zn standard and IRMM Zn metal (table S1).

### Trace element abundances

Whole-rock powders were measured for bulk-rock trace element abundances at the Scripps Isotope Geochemistry Laboratory. Samples were digested at 150°C in Optima-grade concentrated HF (4 ml) and $HNO_3$ (1 ml) for >72 hours on a hot plate, with total analytical blanks and terrestrial basalt standards. Samples were sequentially dried and taken up in concentrated $HNO_3$ to remove fluorides, followed by dilution and doping with indium to monitor instrumental drift during analysis. Trace element abundance analyses were done using a Thermo Scientific iCAP Qc quadrupole inductively coupled plasma mass spectrometer in standard mode. Analyses were standardized versus reference material BHVO-2 that was measured throughout the analytical run. In addition, reference materials were analyzed as "unknowns" (BHVO-2 and BCR-2) to assess matrix matching, external reproducibility, and accuracy. For trace elements, reproducibility of the reference materials was generally better than 5% (relative SD) and in line with standard data measured in the laboratory (*29*).

## SUPPLEMENTARY MATERIALS

Supplementary material for this article is available at http://advances.sciencemag.org/cgi/content/full/3/2/e1602668/DC1

Geological setting, historical background, bomb detonation, and samples
Comparison between trinitite, tektite, and fulgurite
Xenon isotope results
Trace element abundance data
fig. S1. Map of the Trinity test site.
fig. S2. Geology of trinitite.
fig. S3. Images of trinitite samples used in this study.
fig. S4. Upper continental crust–normalized incompatible trace element patterns for trinitite.
fig. S5. Incompatible trace element abundances in trinitite plotted as a function of condensation temperature.
table S1. Zinc abundance and isotopic compositions of trinitite.
table S2. Xenon isotopic compositions of trinitite.
table S3. Trace element abundance data for trinitite samples.
table S4. Mineralogy of trinitite.
table S5. Comparison of trinitite, tektite, and fulgurite formation conditions.
References (*30*–*39*)

## REFERENCES AND NOTES


1. I. H. Campbell, S. R. Taylor, No water, no granites—No oceans, no continents. *Geophys. Res. Lett.* **10**, 1061–1064 (1983).
2. M. M. Hirschmann, Water, melting, and the deep Earth $H_2O$ cycle. *Annu. Rev. Earth Planet. Sci.* **34**, 629–653 (2006).
3. J. F. Kasting, Earth's early atmosphere. *Science* **259**, 920–926 (1993).
4. K. Lodders, Solar system abundances and condensation temperatures of the elements. *Astrophys. J.* **591**, 1220–1247 (2003).
5. B. Marty, The origins and concentrations of water, carbon, nitrogen and noble gases on Earth. *Earth Planet. Sci. Lett.* **313–314**, 56–66 (2012).
6. J. M. D. Day, F. Moynier, Evaporative fractionation of volatile stable isotopes and their bearing on the origin of the Moon. *Philos. Trans. A Math. Phys. Eng. Sci.* **372**, 20130259 (2014).
7. E. D. Young, A. Galy, The isotope geochemistry and cosmochemistry of magnesium. *Rev. Mineral. Geochem.* **55**, 197–230 (2004).
8. R. C. Paniello, J. M. D. Day, F. Moynier, Zinc isotopic evidence for the origin of the Moon. *Nature* **490**, 376–379 (2012).
9. C. Kato, F. Moynier, M. C. Valdes, J. K. Dhaliwal, J. M. D. Day, Extensive volatile loss during formation and differentiation of the Moon. *Nat. Commun.* **6**, 7617 (2015).
10. F. Albarède, E. Albalat, C.-T. A. Lee, An intrinsic volatility scale relevant to the Earth and Moon and the status of water in the Moon. *Meteorit. Planet. Sci.* **50**, 568–577 (2015).
11. Y. Yu, R. H. Hewins, C. M. O. D. Alexander, J. Wang, Experimental study of evaporation and isotopic mass fractionation of potassium in silicate melts. *Geochim. Cosmochim. Acta* **67**, 773–786 (2003).
12. F. M. Richter, R. A. Mendybaev, J. N. Christensen, D. Ebel, A. Gaffney, Laboratory experiments bearing on the origin and evolution of olivine-rich chondrules. *Meteorit. Planet. Sci.* **46**, 1152–1178 (2011).

13. K. Wang, S. B. Jacobsen, Potassium isotopic evidence for a high-energy giant impact origin of the Moon. *Nature* **538**, 487–490 (2016).
14. A. E. Saal, E. H. Hauri, M. L. Cascio, J. A. Van Orman, M. C. Rutherford, R. F. Cooper, Volatile content of lunar volcanic glasses and the presence of water in the Moon's interior. *Nature* **454**, 192–195 (2008).
15. E. H. Hauri, T. Weinreich, A. E. Saal, M. C. Rutherford, J. A. Van Orman, High pre-eruptive water contents preserved in lunar melt inclusions. *Science* **333**, 213–215 (2011).
16. Z. D. Sharp, C. K. Shearer, K. D. McKeegan, J. D. Barnes, Y. Q. Wang, The chlorine isotope composition of the Moon and implications for an anhydrous mantle. *Science* **329**, 1050–1053 (2010).
17. E. Staritzky, *Thermal Effects of Atomic Bomb Explosions on Soils at Trinity and Eniwetok* (LA-1126, Los Alamos Scientific Laboratory, 1950), 16 pp.
18. A. Meshik, O. Pravdivtseva, C. Hohenberg, Fission xenon in trinities from the first nuclear test, in APS April Meeting and HEDP/HEDLA Meeting, St. Louis, MO, 11 to 15 April 2008.
19. G. N. Eby, N. Charnley, D. Pirrie, R. Hermes, J. Smoliga, G. Rollinson, Trinitite redux: Mineralogy and petrology. *Am. Mineral.* **100**, 427–441 (2015).
20. J. J. Bellucci, A. Simonetti, E. C. Koeman, C. Wallace, P. C. Burns, A detailed geochemical investigation of post-nuclear detonation trinitite glass at high spatial resolution: Delineating anthropogenic vs. natural components. *Chem. Geol.* **365**, 69–86 (2014).
21. H. Chen, P. S. Savage, F.-Z. Teng, R. T. Helz, F. Moynier, Zinc isotopic fractionation during magmatic differentiation and the isotopic composition of the bulk Earth. *Earth Planet. Sci. Lett.* **369–370**, 34–42 (2013).
22. E. J. Essene, D. C. Fisher, Lightning strike fusion: Extreme reduction and metal-silicate liquid immiscibility. *Science* **234**, 189–193 (1986).
23. H. E. Belkin, J. W. Horton, Silicate glass and sulphide melts in the ICDP-USGS Eyreville B core, Chesapeake Bay impact structure, Virginia, USA, in *The ICDP-USGS Deep Drilling Project in the Chesapeake Bay Impact Structure: Results from the Eyreville Core Holes*, G. S. Gohn, C. Koeberl, K. G. Miller, W. U. Reimold, Eds. (Geological Society of America Special Paper, 2009), vol. 458, pp. 447–468.
24. J. T. Wasson, W. A. Heins, Tektites and climate. *J. Geophys. Res.* **98**, 3043–3052 (1993).
25. F. Moynier, P. Beck, F. Jourdan, Q.-Z. Yin, U. Reimold, C. Koeberl, Isotopic fractionation of zinc in tektites. *Earth Planet. Sci. Lett.* **277**, 482–489 (2009).
26. F. M. McCubbin, K. E. Vander Kaaden, R. Tartèse, R. L. Klima, Y. Liu, J. Mortimer, J. J. Barnes, C. K. Shearer, A. H. Treiman, D. J. Lawrence, S. M. Elardo, D. M. Hurley, J. W. Boyce, M. Anand, Magmatic volatiles (H, C, N, F, S, Cl) in the lunar mantle, crust, and regolith: Abundances, distributions, processes, and reservoirs. *Am. Mineral.* **100**, 1668–1707 (2015).
27. P. H. Warren, G. J. Taylor, The moon, in *Treatise on Geochemistry*, H. Holland, K. Turekian, Eds. (Elsevier, ed. 2, 2014), pp. 213–250.
28. F. Moynier, M. Le Borgne, High precision zinc isotopic measurements applied to mouse organs. *J. Vis. Exp.* **2015**, e52479 (2015).
29. J. M. D. Day, B. J. Peters, P. E. Janney, Oxygen isotope systematics of South African olivine melilitites and implications for HIMU mantle reservoirs. *Lithos* **202–203**, 76–84 (2014).
30. N. Eby, R. Hermes, N. Charnley, J. A. Smoliga, Trinitite—The atomic rock. *Geology Today* **26**, 181–185 (2010).
31. C. S. Ross, Optical properties of glass from Alamogordo, New Mexico. *Am. Mineral.* **33**, 360–362 (1948).
32. A. J. Fahey, C. J. Zeissler, D. E. Newbury, J. Davis, R. M. Lindstrom, Postdetonation nuclear debris for attribution. *Proc. Natl. Acad. Sci. U.S.A.* **107**, 20207–20212 (2010).
33. T. M. Semkow, P. P. Parekh, D. K. Haines, *ACS Symposium Series 945* (American Chemical Society, 2006), pp. 142–159.
34. R. E. Hermes, W. B. Strickfaden, A new look at trinitite. *Nucl. Weapons J.* **2**, 2–7 (2005).
35. B. Storms, Trinity. *Atom* **2**, 1–34 (1965).
36. M. J. O'Hara, Flood basalts, basalt floods or topless Bushvelds? Lunar petrogenesis revisited. *J. Petrol.* **41**, 1545–1651 (2000).
37. B. P. Glass, F. E. Senftle, D. W. Muenow, K. E. Aggrey, A. N. Thorpe, Atomic bomb glass beads: Tektite and microtektite analogs, in *Proceedings of the Second International Conference on Natural Glasses* (1988), pp. 361–369.
38. A. A. Sheffer M. D. Dyer, $^{57}$Fe Mössbauer spectroscopy of fulgurites: Implications for chemical reduction. *Lunar Planet. Sci.* **35**, 1372 (2004).
39. R. L. Rudnick, S. Gao, Composition of the Continental Crust. *Treatise Geochem.* **3**, 1–64 (2003).

**Acknowledgments:** We thank the two reviewers for their constructive comments. **Funding:** This work was supported by the NASA Emerging Worlds program (NNX15AL74G) and a visiting professor position in the Institut de Physique du Globe de Paris to J.M.D.D. **Author contributions:** J.M.D.D. designed the project and wrote the manuscript. J.M.D.D. and F.M. performed the measurements. A.P.M., O.V.P., and D.R.P. provided the samples, and all authors contributed to the discussion and interpretation of results. **Competing interests:** The authors declare that they have no competing interests. **Data and materials availability:** All data needed to evaluate the conclusions in the paper are present in the paper and/or the Supplementary Materials. All data used in the present article are available by contacting J.M.D.D. (jmdday@ucsd.edu).

Submitted 28 October 2016
Accepted 29 December 2016
Published 8 February 2017
10.1126/sciadv.1602668

**Citation:** J. M. D. Day, F. Moynier, A. P. Meshik, O. V. Pradivtseva, D. R. Petit, Evaporative fractionation of zinc during the first nuclear detonation. *Sci. Adv.* **3**, e1602668 (2017).

# Evaporative fractionation of zinc during the first nuclear detonation

James M. D. Day, Frédéric Moynier, Alex P. Meshik, Olga V. Pradivtseva and Donald R. Petit

*Sci Adv* **3** (2), e1602668.
DOI: 10.1126/sciadv.1602668